THE JOURNAL OF PHYSICAL CHEMISTRY A

Article

pubs.acs.org/JPCA

Improved Flavin-Based Catalytic Photooxidation of Alcohols through Intersystem Crossing Rate Enhancement

Kirill A. Korvinson,[†] George N. Hargenrader,[†] Jelena Stevanovic,[§] Yun Xie,[†] Jojo Joseph,[‡] Veselin Maslak,[§] Christopher M. Hadad,[‡] and Ksenija D. Glusac*[,†]

[†]Department of Chemistry, Center for Photochemical Sciences, Bowling Green State University, Bowling Green, Ohio 43403, United States

[‡]Department of Chemistry and Biochemistry, The Ohio State University, Columbus, Ohio 43210, United States

[§]Faculty of Chemistry, University of Belgrade, Studentski Trg 12-16, Belgrade 11000, Serbia

Supporting Information

ABSTRACT: The triplet excited-state formation efficiency in a flavin derivative was increased by the introduction of iodine into the molecular framework. The transient absorption measurements showed that the intersystem crossing rate was 1.1×10^{10} s^{-1}, significantly faster than in the parent flavin compound. Furthermore, the photocatalytic efficiency of iodoflavin was evaluated using the oxidation of benzyl alcohol as a model reaction. The benzaldehyde product yields were higher when iodoflavin was used as a photocatalyst, showing that the increased triplet yield directly translates into improved photocatalysis. The iodoflavin catalyst also allowed the use of higher substrate concentrations (since the undesired electron transfer from singlet excited state was minimized), which is expected to improve the practical aspects of photocatalysis by flavins.

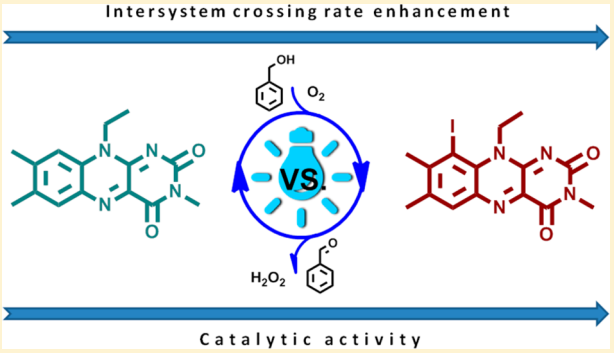

INTRODUCTION

Flavin-based monooxygenases and oxidases are exceptionally efficient in activating molecular oxygen toward catalytic oxidation of a number of organic substrates.[1−6] While monooxygenases insert atomic oxygen into a substrate (S) by catalyzing the reaction involving nicotinamide adenine dinucleotide (NAD) $S + O_2 + NADH + H^+ \rightarrow SO + NAD^+ + H_2O$, the oxidases perform dehydrogenation of the substrate (SH_2) by catalyzing the reaction $SH_2 + O_2 \rightarrow S + H_2O_2$. Given the significance of oxidation reactions in organic syntheses, the artificial biomimetic flavin-based catalysts have been extensively used to oxidize organic compounds by atmospheric oxygen under mild reaction conditions.[7] In the case of oxidase-mimicking catalysts, the oxidative power of the flavin is generally enhanced by photoexcitation. This photoorganocatalytic approach facilitates the oxidation of a number of substrates that cannot be oxidized thermally and has been applied toward the oxidation of aromatic alcohols, amines, and other substrates.[8−15]

Previous mechanistic studies of the photocatalytic oxidations of benzyl alcohols indicate that the first step involves a photoinduced electron transfer from benzyl alcohol to the excited flavin, followed by the proton and hydrogen-atom transfers to generate the oxidized benzylaldehyde product and the reduced flavin FlH_2.[16,17] The subsequent regeneration of the catalyst is achieved by a reaction of FlH_2 with molecular oxygen via the flavin hydroperoxide (FlHOOH) intermediate.[18−20] On the one hand, the initial photoinduced electron transfer from benzyl alcohol can occur to either singlet (S_1) or triplet (T_1) excited states of the flavin. However, a recent study by Riedle and co-workers[17] reported that the electron transfer to the S_1 state is not catalytically productive, as it leads to a fast (~50 ps) back electron transfer. On the other hand, electron transfer to the T_1 state generates long-lived radical ions (~5 μs) that undergo further proton/hydrogen-atom transfers to generate the desired product. Heavy element substituents, such as iodine, are known to increase the S → T intersystem crossing (ISC) rates in organic compounds due to spin−orbit coupling.[21] Given the significance of triplet excited states in flavin-based photocatalysis, the aim of this study was to utilize the heavy-atom effect to increase the quantum yield for the T_1 state formation in flavins. Specifically, it will be shown that the incorporation of the iodine into the flavin framework (I-Fl) leads to a significant increase in the ISC rate relative to the reference compound (Fl, Scheme 1). Furthermore, this manuscript demonstrates that the increased yield of triplet formation in I-Fl directly translates into improved photoorganocatalytic performance relative to the reference model

Received: August 19, 2016
Revised: August 24, 2016
Published: August 26, 2016

DOI: 10.1021/acs.jpca.6b08405
J. Phys. Chem. A 2016, 120, 7294−7300

Scheme 1. General Mechanism for Organocatalytic Photooxidation of Benzyl Alcohol by Flavins

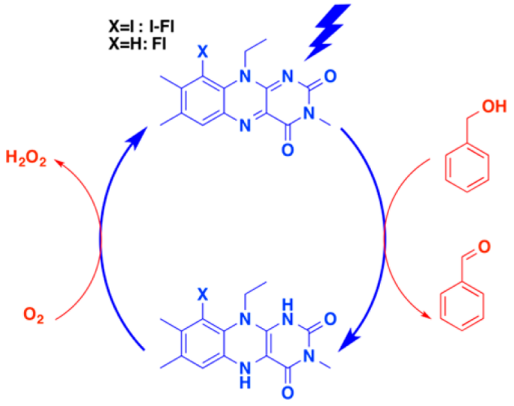

compound. For this purpose, the flavin-catalyzed oxidation of benzyl alcohol to benzaldehyde was used as a model reaction (Scheme 1).

MATERIALS AND METHODS

Unless specified, all reagents, starting materials, and solvents (HPLC grade) were purchased from commercial sources and used as received without purification. ^{1}H and ^{13}C spectra were recorded at ambient temperature on Bruker Avance 300 MHz NMR or Bruker AvanceIII 500 MHz NMR spectrometers. Spectra were described as chemical shifts (ppm), multiplicity (s, singlet; d, doublet; t, triplet; q, quartet; m, multiplet), coupling constant in hertz (Hz), and number of protons. All reactions were monitored using silica gel 60 F_{254} analytical thin-layer chromatography (TLC) plates with UV detection (λ = 254 and 365 nm). Silica gel (60 Å, 40−63 μm) was used as stationary phase for column chromatography.

Synthesis. The isoalloxazine structures of model flavins were synthesized using a condensation between the alloxan and the corresponding aromatic ortho-bis-amine (synthesis of Fl was reported previously).[22,23] The synthesis of I-Fl was performed using the steps presented in Scheme 2.

*6-Iodo-4,5-dimethyl-2-nitroaniline (**2**).* A solution of compound **1** (15 g, 90 mmol), potassium bromate (12 g, 90 mmol), and potassium iodide (15 g, 90 mmol) was prepared in 450 mL of methanol (MeOH)/water (2:3, v/v) mixture. To the resulting solution concentrated hydrochloric acid (37.5 mL, 450 mmol) was added, and the mixture was heated at 60 °C for 4 h. The crude product was extracted with dichloromethane (DCM; 3 × 100 mL), and the organic layer was washed with water, 5% sodium thiosulfate, and brine and dried over sodium sulfate. The solvent was removed under reduced pressure, and the residue was recrystallized from hexane to give 24 g (83 mmol, 80%) of 6-iodo-4,5-dimethyl-2-nitroaniline as an orange solid. Gas chromatography-mass spectrometry (GCMS): m/z found 292 [291.97 calculated for $C_8H_9IN_2O_2$]. ^{1}H NMR (500 MHz, CD_3CN) δ ppm: 7.95 (s, 1H), 6.74 (s, 2H), 2.43 (s, 3H), 2.30 (s, 3H). ^{13}C NMR (500 MHz, CD_3CN) δ ppm: 146.10, 141.12, 130.34, 125, 54, 124.70, 114.24, 20.63, 19.44.

*6-Iodo-N-(4,5-dimethyl-2-nitrophenyl)-2,2,2-trifluoro-acetamide (**3**).* Compound **2** (24 g, 83 mmol) was dissolved in 250 mL of dichloromethane. Triethylamine (9.2 mL, 6.7 g, 165 mmol) and trifluoroacetic anhydride (TFAA; 18.5 mL, 28 g, 133 mmol) were added to the reaction mixture and stirred for 4 h. Solution was transferred to a separatory funnel and washed once with 150 mL of 2 M hydrochloric acid, three times with 100 mL portions of 2 M sodium bicarbonate, and once with brine. The organic fraction was dried over anhydrous calcium chloride, and the excess solvent was evaporated. The product was purified using flash chromatography (hexane/ethyl acetate (EtOAc) = 6:1) to give 28 g (72 mmol, 87%) of pure compound **3** as a white solid. GCMS: m/z found 388 [387.95 calculated for $C_{10}H_8F_3IN_2O_3$]. ^{1}H NMR (500 MHz, CD_3CN) δ ppm: 9.38 (s, 1H), 7.89 (s, 1H), 2, 50 (s, 3H), 2.45 (s, 3H). ^{13}C NMR (500 MHz, CD_3CN) δ ppm: 156.7 (q, J^{C-F} = 155 Hz), 145.79, 141.30, 127.67, 125.98, 125.12, 21.35, 21.33.

*6-Iodo-N-ethyl-N-(4,5-dimethyl-2-nitro-phenyl)-amine (**4**).* Compound **3** (27 g, 70 mmol) was dissolved in 150 mL of dimethylformamide (DMF); anhydrous potassium carbonate (19 g, 140 mmol) and 3.2 mL of ethyl iodide (EtI; 15 mL, 30 g, 190 mmol) were added, and the mixture was stirred for 26 h at 60 °C. Once the conversion was completed, 100 mL of 10% solution of NaOH in methanol/water (1:1) was added. The mixture was heated at 65 °C for 3 h, cooled to room temperature, and extracted with dichloromethane; the organic layer was dried over calcium chloride, and the solvent was evaporated under reduced pressure. The crude product was purified by flash chromatography (hexane/ethyl acetate, 10:1) to give 16 g (50 mmol, 72%) of compound **4** as a bright orange oil, which crystallized upon cooling. GCMS: m/z found 320 [320.00 calculated for $C_{10}H_{13}IN_2O_2$]. ^{1}H NMR (500 MHz, CD_3CN) δ ppm: 7.67 (s, 1H), 5.54 (s, 1H), 3.13 (q, J = 10 Hz, 2H), 2.41 (s, 3H), 2.29 (s, 3H), 1.15 (t, J = 10 Hz, 3H). ^{13}C

Scheme 2. Synthesis[a] of I-Fl

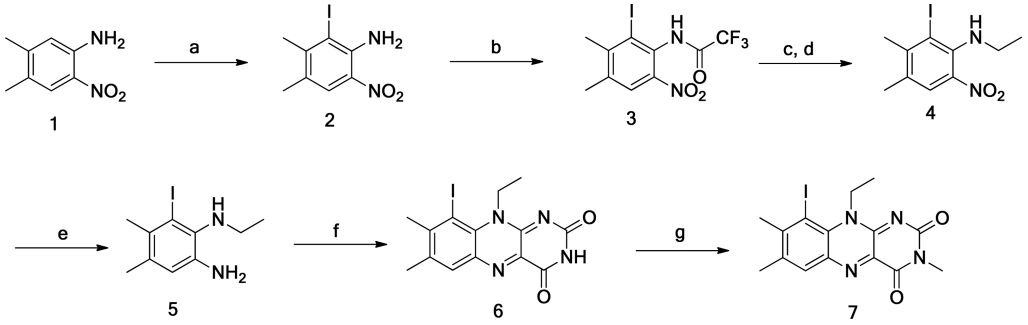

[a](a) KBr-O_3, potassium iodide (Kl), HCl, MeOH/H_2O, 60 °C, 4 h, 92%; (b) trifluoroacetic anhydride (TFAA), Et_3N, dichloromethane (DCM), 4 h, 82%; (c) ethyl iodide (Etl), K_2CO_3, dimethylformamide (DMF), 60 °C, 26 h; (d) NaOH, MeOH/H_2O, 65 °C, 3h, 76%; (e) Sn, HCl, 95 °C, 2 h, 32%; (f) aloxane monohydrate, $B(OH)_3$, acetic acid (AcOH0, 10 h 67%; (g) methyl iodide (Mel), K_2CO_3, DMF, 72 h, 87%.

DOI: 10.1021/acs.jpca.6b08405
J. Phys. Chem. A 2016, 120, 7294−7300

NMR (500 MHz, CD_3CN) δ ppm: 145.41, 141.78, 129.57, 126.12, 119.67, 43.45, 21.59, 20.53, 16.09.

*6-Iodo-N-ethyl-4,5-dimethyl-benzene-1,2-diamine (**5**).* Compound **4** (15 g, 47 mmol) was partially dissolved in 250 mL of 12 M HCl. The reaction mixture was heated to 95 °C, and tin foil (27 g, 230 mmol) in small amounts was added to the reaction mixture until solution became colorless. The reaction mixture was cooled, and 6 M NaOH was added dropwise until the pH of the mixture became 10. The formed suspension was heated and passed through a bed of diatomaceous earth. The filtrate was extracted with dichloromethane; the organic layer was dried over sodium sulfate and evaporated under reduced pressure. Crude product was purified using column chromatography (ethyl acetate/hexane 1:9) to give 4.13 g (15 mmol, 32%) of compound **5** as a brown oil. GCMS: m/z found 290 [290.03 calculated for $[C_{10}H_{15}IN_2]$. ^{1}H NMR (500 MHz, CD_3CN) δ ppm: 6.50 (s, 1H), 4.10 (s, 2H), 3.25 (s, 1H), 2.85 (q, J = 5 Hz, 2H), 2.23 (s, 3H), 2.17 (s, 3H), 1.15 (t, J = 7.5, 3H). ^{13}C NMR (500 MHz, CD_3CN) δ ppm: 141.83, 133.93, 131.97, 125.12, 124.27, 116.68, 42.27, 21.01, 19.65, 16.06.

*10-Ethyl-9-iodo-7,8-dimethylbenzo[g]pteridine-2,4-(3H,10H)-dione (**6**).* Compound **5** (3.5 g, 12.7 mmol) was added dropwise to the suspension of alloxan monohydrate (4.1 g, 25.4 mmol) and boric acid (0.4 g, 6.4 mmol) in 20 mL of glacial acetic acid. The mixture was stirred overnight, and the precipitate was filtered off and recrystallized from methanol to give 3.4 g (8.5 mmol, 67%) of compound **6** as a yellow solid. Matrix-assisted laser desorption/ionization mass spectrometry (MALDI MS), m/z found: 396 [396.01 calculated for $C_{14}H_{13}IN_4O_2$]. ^{1}H NMR (500 MHz, deuterated dimethyl sulfoxide (DMSO-d_6)) δ ppm: 11.44 (s, 1H), 7.92 (s, 1H), 4.82 (q, J = 7.5, 2H), 2.60 (s, 3H), 2.49 (s, 3H), 1.55 (t, J = 7.5, 3H). ^{13}C NMR (500 MHz, DMSO-d_6) δ ppm: 159.61, 155.64, 152.78, 146.76, 138.09, 136.13, 135.39, 131.59, 131.49, 110.82, 45.76, 22.38, 20.71, 14.55.

*I-Fl (10-Ethyl-9-iodo-3,7,8-trimethylbenzo[g]pteridine-2,4-(3H,10H)-dione) (**7**).* Compound **6** (3 g, 7.6 mmol) was partially dissolved in 50 mL of dry DMF, and then K_2CO_3 (5.3 g, 38 mmol) and iodomethane (2.4 mL, 5.4 g, 38 mmol) were added. The mixture was stirred at room temperature for 3 d. Brine (~100 mL) was added to the solution, and the mixture was extracted with dichloromethane. Crude product was purified by flash chromatography (acetone/DCM = 1:2) to give 2.6 g (6.3 mmol, 83%) of I-Fl as an orange solid. MALDI MS, m/z found: 410.14 [410.02 calculated for $C_{15}H_{15}IN_4O_2$]. ^{1}H NMR (500 MHz, DMSO-d_6) δ ppm: 7.99 (s, 1H), 4.87 (q, J = 7.5, 2H), 3.27 (s, 3H), 2.61 (s, 3H), 1.55 (t, J = 7.5, 3H). ^{13}C NMR (500 MHz, DMSO-d_6) δ ppm: 159.85, 155.62, 151.72, 147.41, 137.68, 136.69, 136.03, 132.02, 131.89, 111.20, 45.92, 28.36, 22.86, 21.16, 15.01.

Femtosecond Transient Absorption Experiments. The laser system for the femtosecond transient absorption measurements was described previously.[24] Briefly, the 800 nm laser pulses were produced at a 1 kHz repetition rate (full width at half-maximum (fwhm) = 110 fs) by a mode-locked Ti:sapphire laser (Hurricane, Spectra-Physics). The output from the Hurricane was split into pump (85%) and probe (10%) beams. The pump beam (800 nm) was sent into an optical parametric amplifier (OPA-400, Spectra Physics) to obtain the 480 nm pump pulses (E < 1 μJ/pulse). The probe beam was focused into a horizontally moving CaF_2 crystal for white light continuum generation between 350 and 800 nm. The relative polarization between the pump and the probe beams was set at the magic angle (54.7°). The pump and probe beams were overlapped in the sample. The flow cell (Starna Cell Inc. 45-Q-2, 0.9 mL volume with 2 mm path length), pumped by a Fluid Metering RHSY Lab pump (Scientific Support Inc), was used to prevent photodegradation of the sample. After passing through the cell, the continuum was coupled into an optical fiber and input into a CCD spectrograph (Ocean Optics, S2000). The data acquisition was achieved using in-house LabVIEW (National Instruments) software routines. The group velocity dispersion of the probing pulse was determined using nonresonant optical Kerr effect (OKE) measurements. Sample solutions were prepared at a concentration needed to have absorbance of $A \approx 0.6-1.0$ at the excitation wavelength.

Nanosecond Transient Absorption Experiments. The nanosecond laser flash photolysis experimental setup utilized for the measurements in this paper is described in detail elsewhere.[25] Briefly, a Nd:YAG laser (Spectra Physics LAB-150−10) was used as the excitation light source with an excitation wavelength of 355 nm. The probe light was supplied by a 150 W xenon arc lamp (Applied Photophysics) used in pulsed mode (0.5 ms in duration) with a 1 Hz repetition rate. Transient absorption spectra were recorded using a Roper ICCD-Max 512T digital intensified CCD camera with up to 2 ns temporal resolution. The single-wavelength kinetics measurements were recorded using a photomultiplier tube connected to an oscilloscope (Tektronix TDS 680C 5Gs/s 1 GHz), which was connected to a computer that runs a custom LabView control and acquisition program. Sample solutions were prepared at a concentration needed to have absorbance of $A \approx 0.5-0.8$ at the excitation wavelength (355 nm). Solutions were placed in a quartz cuvette and deoxygenated prior to nanosecond transient absorption experiments by purging with argon.

Photocatalysis. A 10 mL vial was charged with the catalyst (1−10 mol %), thiourea (15 mol %, if needed), and 3 mL of solvent. The resulting mixture was stirred in the dark until all reagents dissolved. Then BnOH (1 equiv) was added, and the vial was placed under a 12 W light-emitting diode (LED) lamp (λ = 440 nm). Reaction mixture was stirred for the required time while being monitored by TLC and ^{1}H NMR methods. The Supporting Information contains the representative NMR spectra (Figures S1 and S2).

Example (Table 1, Entry 13). A 10 mL vial was charged with I-Fl (11 mg, 27 μmol), thiourea (31 mg, 0.41 mmol), and 3 mL of 5% DMSO-d_6 in deuterated acetonitrile (ACN-d_3). The mixture was stirred in the dark for 5 min. Then BnOH (292 mg, 0.28 mL, 2.7 mmol) was added, and the vial was placed under a 12 W LED lamp (λ = 440 nm). Reaction mixture was stirred for 5 h until full conversion of the starting alcohol was detected. A 50 μL aliquot of the mixture was diluted to 0.5 mL and analyzed by ^{1}H NMR to show 98% yield of benzaldehyde (1,3,5-trimethoxybenzene as a standard). See Table 1, entry 13 for data.

Photostability Test. Oven-dried vial was charged with solution of BnOH in 5% DMSO-d_6 in CD_3CN (4.7×10^{-3} M, 3 mL), standard, magnetic stirrer bar, and thiourea (15 mol %). Then, the catalyst (10 mol %) was added, and the mixture was stirred in the dark until all reagents were dissolved. The vial was placed under LED (440 nm, 12W), and the mixture was stirred under light. Reactions were monitored by TLC. Once reaction was complete (155 min for Fl and 90 min for I-Fl), the product

DOI: 10.1021/acs.jpca.6b08405
J. Phys. Chem. A 2016, 120, 7294−7300

Table 1. Catalytic Photooxidation with Flavins

entry	catalyst, mol %	solvent	time, h	yield,[b] %
1	Fl (10)	5% DMSO in ACN	1.5	31
2	I-Fl (10)	5% DMSO in ACN	1.5	42
3	Fl (10)	5% DMSO in H_2O	1.5	41
4	I-Fl (10)	5% DMSO in H_2O	1.5	54
5	Fl (10)	ACN/H_2O (1:2)	1.5	77
6	I-Fl (10)	ACN/H_2O (1:2)	1.5	89
7[c]	Fl (10)	5% DMSO in ACN	1.5	72
8[c]	I-Fl (10)	5% DMSO in ACN	1.5	>95
9[c]	Fl (10)	5% DMSO in ACN	2.5	>95
10[c]	Fl (1)	5% DMSO in ACN	12	48
11[c]	I-Fl (1)	5% DMSO in ACN	12	54
12[c,d]	Fl (1)	5% DMSO in ACN	5	21
13[c,d]	I-Fl (1)	5% DMSO in ACN	5	>95

[a]Conditions: benzyl alcohol 4.5 × 10^{-3} M. [b]NMR yields; 1,3,5-trimethoxybenzene as a standard. [c]Thiourea 15 mol %. [d]0.9 M BnOH.

yield was determined using NMR (1,3,5-trimethoxybenzene was used as an internal standard). Then, another portion of neat alcohol was added to the mixture, and the procedure was repeated for additional cycle. For every additional cycle, the amount of BnOH to be added was calculated based on NMR yields to match the initial concentration of 4.7 mmol.

RESULTS AND DISCUSSIONS

The UV/vis absorption spectra of Fl and I-Fl (Figure 1a) are similar, with two absorption bands at ~350 and 450 nm arising

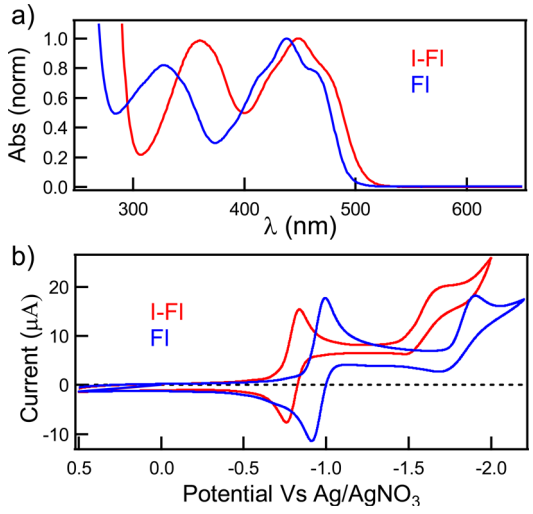

Figure 1. (a) Absorption spectra of Fl (blue) and I-Fl (red) in acetonitrile; (b) cyclic voltammograms of Fl (blue) and I-Fl (red) in 0.1 M tetrabutylammonium perchlorate in acetonitrile (Pt working electrode, 0.1 V/s scan rate). The first reduction potentials are at −0.95 V (Fl) and −0.85 V (I-Fl) vs $Ag/AgNO_3$.

due to π,π^* electronic transitions.[22] The spectral similarity indicates that Fl and I-Fl have almost equal capacity to drive useful photochemical transformations using the energy of blue photons. The standard reduction potentials for Fl and I-Fl were obtained using cyclic voltammetry (Figure 1b). Both model compounds exhibit two reduction peaks associated with the formation of the semiquinone and hydroquinone forms of the flavin.[22] The I-Fl reduces at a more positive potential, indicating that it is a better electron acceptor. Assuming that the triplet excited-state energies of Fl and I-Fl are the same, this implies that the driving force for the photoinduced electron transfer from T_1 state of I-Fl to the substrate is, by 0.15 eV, larger than the corresponding driving force for Fl.

Femtosecond pump−probe experiments were performed to evaluate the ISC rates in model flavins. The transient spectra collected at early times are assigned to the $^1\pi,\pi^*$ states of Fl and I-Fl (Figure 2a) and consist of the ground-state bleach (400−

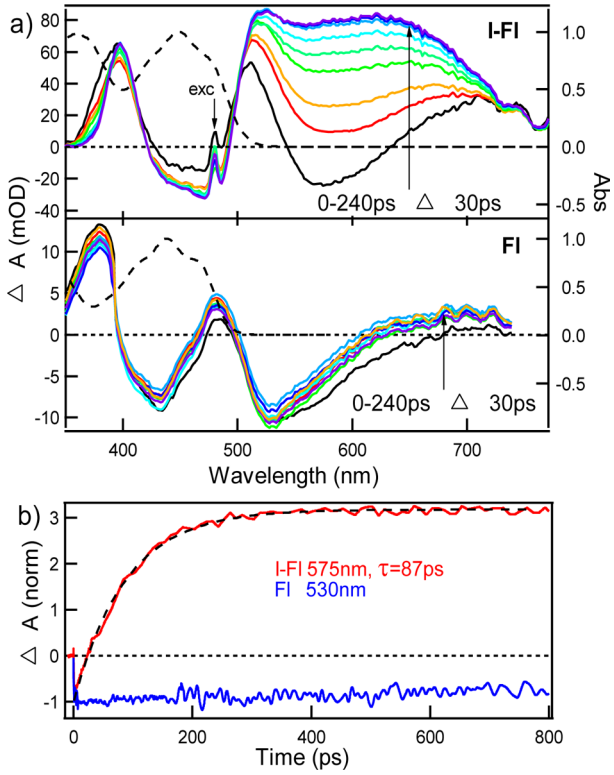

Figure 2. (a) Transient absorption difference spectra of I-Fl (upper) and Fl (lower) in ACN collected 0−240 ps after the 480 nm excitation pulse. The ground-state absorption spectra of Fl and I-Fl are presented as dashed curves for comparison. (b) Kinetics profiles for I-Fl, probed at 575 nm (red) with exponential fit (dashed), and Fl, probed at 530 nm (blue).

500 nm), stimulated emission (500−700 nm), and excited-state absorption (350−400 nm and ~500 nm) bands. The lifetimes of these $^1\pi,\pi^*$ states are significantly different in the two model compounds: in the case of Fl, the $^1\pi,\pi^*$ state decays within several nanoseconds to form the $^3\pi,\pi^*$ state,[22] while the spin inversion occurs with a lifetime of only 87 ps for I-Fl (Figure 2b). The formation of the $^3\pi,\pi^*$ state of I-Fl is observed as growths of absorption bands at 400 nm and in the 500−700 nm range. The significantly faster ISC rate and the absence of ground-state bleach recovery in the case of I-Fl demonstrates that the incorporation of iodine provides an efficient route toward increased triplet-state quantum yields in flavin derivatives.

The lifetimes of the triplet excited states in Fl and I-Fl were evaluated using nanosecond transient absorption spectroscopy (Figure 3). The $^3\pi,\pi^*$ states of Fl and I-Fl exhibit broad absorption features that cover the entire visible range (Figure 3a). Both triplets decay on the microsecond time scale, as can be observed from the kinetics traces probed at 600 nm (Figure 3b). The triplet excited lifetime of I-Fl is somewhat shorter (5.8

DOI: 10.1021/acs.jpca.6b08405
J. Phys. Chem. A 2016, 120, 7294−7300

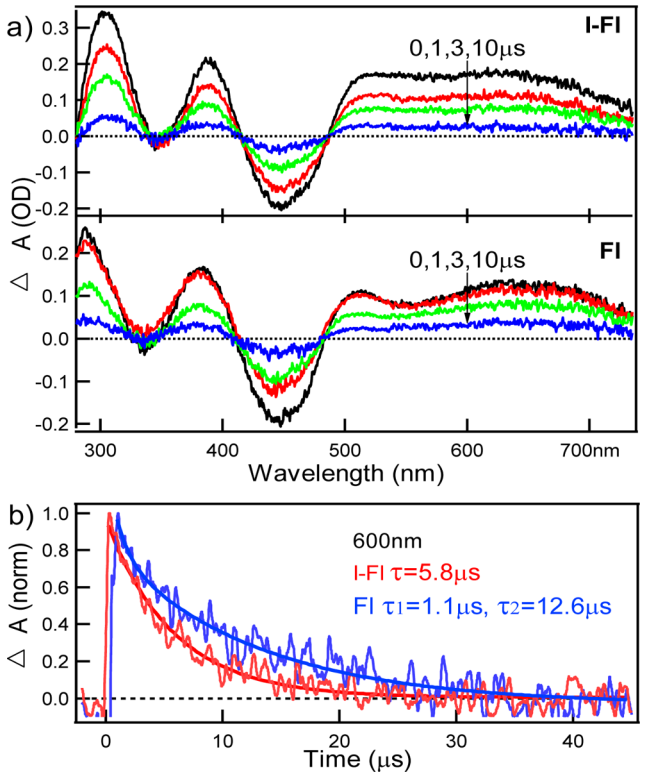

Figure 3. (a) Transient absorption difference spectra of I-Fl (upper) and Fl (lower) in ACN collected from 0 to 10 μs after the 355 nm excitation pulse. (b) Kinetics profiles for I-Fl (red) and Fl (blue) probed at 600 nm.

μs) than the lifetime of the corresponding triplet in Fl (12.6 μs). Even though the kinetics traces obtained in Figure 3b were obtained using the lowest possible power of the pump beam, it is possible that the lifetimes are affected by the bimolecular annihilation processes.[26] The shortening of the triplet excited-state lifetime in I-Fl is consistent with the heavy atom effect caused by the iodo-substituent: the spin−orbit interaction in I-Fl causes not only an increase in the rate of $S_1 \rightarrow T_1$ ISC (Figure 2b) but also leads to increased rate of the $T_1 \rightarrow S_0$ relaxation pathway (Figure 3b). Importantly, this heavy-atom effect is much more pronounced in accelerating the $S_1 \rightarrow T_1$ process (ISC rate in I-Fl is ∼100 times higher than in Fl, Figure 2b) than in accelerating the $T_1 \rightarrow S_0$ relaxation (rate is only ∼2 times faster, Figure 3b). Such situation is ideal for promoting the photocatalytic processes using triplet excited state of flavin, where one needs high triplet quantum yields (which is assured with fast ISC rates) and long triplet excited-state lifetimes, thus providing sufficient time for the photochemical event to take place.

The photocatalytic efficiency of I-Fl was evaluated using the oxidation of benzyl alcohol as a model reaction (Scheme 3). The catalysis was evaluated in three solvent mixtures: DMSO/ACN, DMSO/H_2O, and ACN/H_2O (Table 1). The product

Scheme 3. Organocatalytic Photooxidation of Benzyl Alcohol

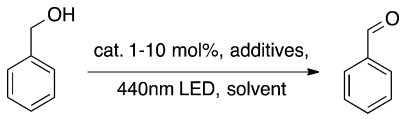

yields were highest in the ACN/H_2O solvent mixture (for example, compare entries 2, 4, and 6), which is consistent with the previous reports showing that the higher-polarity solvents more efficiently stabilize the radical ions formed after the photoinduced electron transfer.[16] The addition of thiourea as an electron mediator[10] significantly increases the benzaldehyde yield (e.g., compare entries 2 and 8). In addition, the 10 mol % catalyst loading gives higher benzaldehyde yields (entry 8) than the 1 mol % loading (entry 11). Importantly, the comparison of Fl and I-Fl photocatalysis revealed that I-Fl provided consistently higher benzaldehyde yields. For example, entries 7 and 8 report two reactions in which all experimental conditions were identical, except that different catalysts were used. While the I-Fl catalyst provided a 100% yield of benzaldehyde, the yield in the presence of Fl was only 72%. These results are consistent with the previous report[17] showing that the efficient catalysis occurs from the triplet excited state of flavin, while the singlet excited state leads to undesired charge recombination process. Since the iodine in I-Fl provides higher triplet quantum yield and lower singlet excited-state lifetime, the photocatalysis is more efficient for I-Fl.

Furthermore, the use of I-Fl as a photocatalyst allows the use of higher concentrations of the benzyl alcohol substrate. To avoid the unwanted charge recombination that occurs from the singlet excited-state pathway, the catalysis by flavins is optimal when lower concentrations of reactant are used (highest yields were obtained at 25 mM substrate concentration).[17] Similar behavior was observed in this work: when benzyl alcohol concentration was increased from 4.5 mM to 0.9 M, the product yield in the presence of Fl as a catalyst decreased from 48 to 21% (entries 10 and 12). The opposite results were obtained when I-Fl was used as a catalyst (entries 11 and 13), where almost quantitative conversion occurred at 0.9 M substrate concentration. The improved catalytic efficiency of I-Fl at high substrate concentration is expected to facilitate the scale-up of the flavin-based photooxidation reactions.

The photocatalytic performance of I-Fl was compared to that of Fl by evaluating the time it takes to bring the BnOH oxidation to completion. In the case of Fl, the reaction took 155 min, while I-Fl photocatalysis required only 90 min under identical experimental conditions (entry 1, Figure 4). There results indicate that the quantum yield for I-Fl catalysis is higher than for Fl, and the results are consistent with the higher photoreactivity of the triplet excited state. However, subsequent addition of BnOH to the reaction mixture (entries 2−4, Figure 4) led to a decrease in oxidation yields for both Fl and I-Fl, indicating that the model flavin catalysts undergo photo-decomposition. In the case of I-Fl, the photo-decomposition was more pronounced, as evidenced by a more drastic decrease in the product yields. It appears that the triplet excited state in I-Fl is responsible for the unwanted photochemical reaction that causes the catalyst decomposition.

To evaluate the energetics for the photoinduced charge transfer from excited Fl and I-Fl, a diagram showing the reduction potentials of excited flavin models is shown in Scheme 4. The reported potentials are only estimates rather than the exact values, because the standard reduction potential of benzyl alcohol radical cation ($BnOH^{\cdot+}$) is not known (instead, anodic peak potential for BnOH oxidation was used[27]) and because the reduction potentials for the flavin models in their T_1 state were obtained under assumption that their triplet energies are the same as that of riboflavin.[28] Despite these possible sources of error, it appears that the photoinduced

DOI: 10.1021/acs.jpca.6b08405
J. Phys. Chem. A 2016, 120, 7294−7300

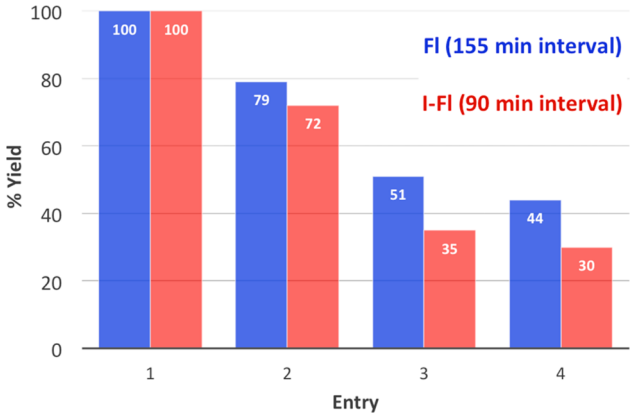

Figure 4. Yields of benzaldehyde formed using Fl (blue) or I-Fl (red) as a photocatalyst. The BnOH oxidation was performed until all alcohol was converted to aldehyde (which took 155 min for Fl and 90 min for I-Fl). Then, a new portion of BnOH was added, and the procedure was repeated in the same time interval. The reactions were performed in 5% DMSO-d_6 in CD_3CN and in the presence of 15 mol % urea.

Scheme 4. Diagram Showing the Standard Reduction Potentials of Relevant Species[a]

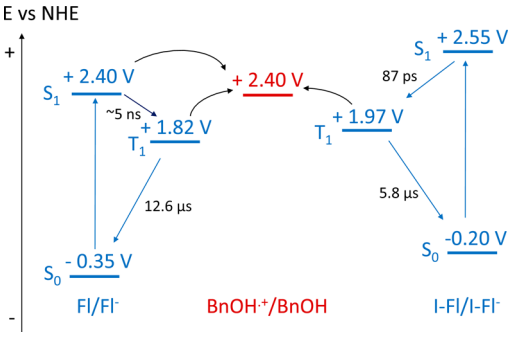

[a]The standard reduction potentials of Fl and I-Fl in their ground states were obtained from the cyclic voltammograms in Figure 1b. The corresponding potentials in the S_1 states were obtained using the energies of the lowest absorption bands shown in Figure 1a. The potentials in the T_1 states were obtained assuming the triplet energy of riboflavin (2.17 eV).[28] For the oxidation potential of BnOH, the anodic peak potential value for a chemically irreversible oxidation was used[27].

electron transfer is thermodynamically favorable only for the flavins in their singlet excited state. Surprisingly, the reduction potentials of Fl and I-Fl in their triplet states are significantly below the oxidation potential of BnOH, making it unlikely that the photoinduced electron transfer from T_1 states of flavins to BnOH is taking place. On the basis of these thermodynamic arguments, we postulate that the photooxidation of BnOH proceeds by a hydrogen atom transfer mechanism. However, further time-resolved experiments are needed to provide more insights into this process.

CONCLUSION

In conclusion, the iodosubstituted flavin was synthesized and shown to exhibit higher rate of triplet formation and improved photocatalytic efficiency. These results verify that the triplet excited state of flavin plays an important role in photocatalytic oxidations of organic substrates. Our findings are expected to contribute to the current research efforts in the area of photocatalytic organic synthesis.[29−31] Furthermore, the iodoflavin analogue reported here will likely find applications in biological sciences, as an artificial cofactor for photoactive flavoproteins.[32−34]

ASSOCIATED CONTENT

Supporting Information

The Supporting Information is available free of charge on the ACS Publications website at DOI: 10.1021/acs.jpca.6b08405.

Photocatalysis data (PDF)

AUTHOR INFORMATION

Corresponding Author

*E-mail: kglusac@bgsu.edu.

Funding

We are grateful to the National Science Foundation (CHE-1055397 to K.D.G. and DMR-1212842 to C.M.H.) for funding this work.

Notes

The authors declare no competing financial interest.

REFERENCES

(1) Huijbers, M. M. E.; Montersino, S.; Westphal, A. H.; Tischler, D.; van Berkel, W. J. H. Flavin Dependant Monooxygenases. *Arch. Biochem. Biophys.* **2014**, *544*, 2.

(2) Mansoorabadi, S. O.; Thibodeaux, C. J.; Liu, H. W. The Diverse Roles of Flavin Coenzymess - Nature's Most Versatile Thespians. *J. Org. Chem.* **2007**, *72*, 6329.

(3) Gadda, G. Hydride Transfer Made Easy in the Reaction of Alcohol Oxidation Catalyzed by Flavin-dependent Oxidases. *Biochemistry* **2008**, *47*, 13745.

(4) Schaefer-Ramadan, S.; Gannon, S. A.; Thorpe, C. Human Augmenter of Liver Regeneration: Probing the Catalytic Mechanism of a Flavin-Dependent Sulfhydryl Oxidase. *Biochemistry* **2013**, *52*, 8323.

(5) Fagan, R. L.; Palfey, B. A. In *Comprehensive Natural Products II;* Liu, H.-W., Mander, L., Eds.; Elsevier: Oxford, U.K, 2010; p 37.

(6) Cashman, J. R.; Motika, M. S. In *Comprehensive Toxicology,* 2nd ed.; McQueen, C. A., Ed.; Elsevier: Oxford, U.K, 2010; p 77.

(7) Iida, H.; Imada, Y.; Murahashi, S. I. Biomimetic Flavin-Catalysed Reactions for Organic Synthesis. *Org. Biomol. Chem.* **2015**, *13*, 7599.

(8) Lechner, R.; Kümmel, S.; König, B. Visible Light Flavin Photo-Oxidation of Methylbenzenes, Styrenes and Phenylacetic Acids. *Photochem. Photobiol. Sci.* **2010**, *9*, 1367.

(9) Schmaderer, H.; Hilgers, P.; Lechner, R.; König, B. Photooxidation of Benzyl Alcohols with Immobilized Flavins. *Adv. Synth. Catal.* **2009**, *351*, 163.

(10) Svoboda, J.; Schmaderer, H.; König, B. Thiourea-Enhanced Flavin Photooxidation of Benzyl Alcohol. *Chem. - Eur. J.* **2008**, *14*, 1854.

(11) Fukuzumi, S.; Kuroda, S. Photooxidation of Benzyl Alcohol Derivatives By Oxygen, Catalyzed By Protonated Flavin Analogues. *Res. Chem. Intermed.* **1999**, *25*, 789.

(12) Fukuzumi, S.; Yasui, K.; Suenobu, T.; Ohkubo, K.; Fujitsuka, M.; Ito, O. Efficient Catalysis of Rare-Earth Metal Ions in Photoinduced Electron-Transfer Oxidation of Benzyl Alcohols by a Flavin Analogue. *J. Phys. Chem. A* **2001**, *105*, 10501.

(13) Tong, W.; Ye, H. P.; Zhu, H. H.; D'Souza, V. T. Photooxidation of Substituted Benzyl Alcohol by Riboflavin. *J. Mol. Struct.: THEOCHEM* **1995**, *333*, 19.

(14) Fukuzumi, S.; Tanii, K.; Tanaka, T. Protonated Pteridine and Flavin Analogues acting as Efficient and Substrate-selective Photocatalysts in the Oxidation of Benzyl Alcohol Derivatives by Oxygen. *J. Chem. Soc., Chem. Commun.* **1989**, 816.

DOI: 10.1021/acs.jpca.6b08405
J. Phys. Chem. A 2016, 120, 7294−7300

(15) Haas, W.; Hemmerich, P. Flavin-Dependent Substrate Photooxidation as a Chemical Model of Dehydrogenase Action. *Biochem. J.* **1979**, *181*, 95.
(16) Feldmeier, C.; Bartling, H.; Magerl, K.; Gschwind, R. M. LED-Illuminated NMR Studies of Flavin-Catalyzed Photooxidations Reveal Solvent Control of the Electron-Transfer Mechanism. *Angew. Chem., Int. Ed.* **2015**, *54*, 1347.
(17) Megerle, U.; Wenninger, M.; Kutta, R. J.; Lechner, R.; König, B.; Dick, B.; Riedle, E. Unraveling the Flavin-catalyzed Photooxidation of Benzylic Alcohol with Transient Absorption Spectroscopy from Subpico- to Microseconds. *Phys. Chem. Chem. Phys.* **2011**, *13*, 8869.
(18) Gelalcha, F. G. Heterocyclic Hydroperoxides in Selective Oxidations. *Chem. Rev.* **2007**, *107*, 3338.
(19) Massey, V. Activation of Molecular Oxygen by Flavins and Flavoprotein. *J. Biol. Chem.* **1994**, *269*, 22459.
(20) Frederick, R. E.; Mayfield, J. A.; DuBois, J. L. Regulated O_2 Activation in Flavin-Dependent Monooxygenases. *J. Am. Chem. Soc.* **2011**, *133*, 12338.
(21) Koziar, J. C.; Cowan, D. O. Photochemical Heavy-atom Effects. *Acc. Chem. Res.* **1978**, *11*, 334.
(22) Sichula, V.; Kucheryavy, P.; Khatmullin, R.; Hu, Y.; Mirzakulova, E.; Vyas, S.; Manzer, S. F.; Hadad, C. M.; Glusac, K. D. Electronic Properties of N(5)-Ethyl Flavinium Ion. *J. Phys. Chem. A* **2010**, *114*, 12138.
(23) Mirzakulova, E.; Khatmullin, R.; Walpita, J.; Corrigan, T.; Vargas-Barbosa, N. M.; Vyas, S.; Oottikkal, S.; Manzer, S. F.; Hadad, C. M.; Glusac, K. D. Electrode-assisted Catalytic Water Oxidation by a Flavin Derivative. *Nat. Chem.* **2012**, *4*, 794.
(24) Li, G.; Glusac, K. D. Light-Triggered Proton and Electron Transfer in Flavin Cofactors. *J. Phys. Chem. A* **2008**, *112*, 4573.
(25) Martin, C. B.; Tsao, M. L.; Hadad, C. M.; Platz, M. S. The Reaction of Triplet Flavin with Indole. A Study of the Cascade of Reactive Intermediates Using Density Functional Theory and Time Resolved Infrared Spectroscopy. *J. Am. Chem. Soc.* **2002**, *124*, 7226.
(26) Yoshimura, A.; Ohno, T. Quenching of Excited Triplet Lumiflavin by Lumiflavin Radicals Formed in its T-T Reaction. *Photochem. Photobiol.* **1991**, *53*, 175.
(27) Higashimoto, S.; Suetsugu, N.; Azuma, M.; Ohue, H.; Sakata, Y. Efficient and Selective Oxidation of Benzylic Alcohol by O2 into Corresponding Aldehydes on a TiO2 Photocatalyst Under Visible Light Irradiation: Effect of Phenyl-ring Substitution on the Photocatalytic Activity. *J. Catal.* **2010**, *274*, 76.
(28) Murov, S. L.; Carmichael, I.; Hug, G. L. *Handbook of Photochemistry,* 2nd ed.; CRC Press: New York, 1993.
(29) Prier, C. K.; Rankic, D. A.; MacMillan, D. W. Visible Light Photoredox Catalysis with Transition Metal Complexes: Applications in Organic Synthesis. *Chem. Rev.* **2013**, *113*, 5322.
(30) Yoon, T. P.; Ischay, M. A.; Du, J. Visible Light Photocatalysis as a Greener Approach to Photochemical Synthesis. *Nat. Chem.* **2010**, *2*, 527.
(31) Hamilton, D. S.; Nicewicz, D. A. Direct Catalytic Anti-Markovnikov Hydroetherification of Alkenols. *J. Am. Chem. Soc.* **2012**, *134*, 18577.
(32) Brust, R.; Lukacs, A.; Haigney, A.; Addison, K.; Gil, A.; Towrie, M.; Clark, I. P.; Greetham, G. M.; Tonge, P. J.; Meech, S. R. Proteins in Action: Femtosecond to Millisecond Structural Dynamics of a Photoactive Flavoprotein. *J. Am. Chem. Soc.* **2013**, *135*, 16168.
(33) Sancar, A. Cryptochrome: The Second Photoactive Pigment in the Eye and Its Role in Circadian Photoreception. *Annu. Rev. Biochem.* **2000**, *69*, 31.
(34) Zhong, D.; Zewail, A. H. Femtosecond Dynamics of Flavoproteins: Charge Separation and Recombination in Riboflavine (Vitamin B_2)-Binding Protein and in Glucose Oxidase Enzyme. *Proc. Natl. Acad. Sci. U. S. A.* **2001**, *98*, 11867.

DOI: 10.1021/acs.jpca.6b08405
J. Phys. Chem. A 2016, 120, 7294−7300